

washed with HCl (pH = 2), dried over MgSO<sub>4</sub>, and then chromatographed on silica gel plates with CH<sub>2</sub>Cl<sub>2</sub> as eluent to give the acetylenic ligand **III** (350 mg, 1.3 mmol; 52% yield). <sup>1</sup>H NMR (δ in ppm, CCl<sub>3</sub>): 7.57 (multiplet), -H aromatic; 6.63 (singlet), -H vinylic; 4.72 (singlet), -NH; 3.96 (doublet of doublets, <sup>3</sup>J = 8.7 Hz, <sup>4</sup>J = 2.5 Hz), -CH<sub>2</sub>; 2.15 (triplet, <sup>4</sup>J = 2.5 Hz), -HC≡C. IR ( $\bar{\nu}$  in cm<sup>-1</sup>, KBr disk): 3429 m, 3288 m, 3022 m, 2922 m, 2115 w, 1668 s, 1404 s.† UV (λ in nm, MeOH): 284 m, 237 m, 216 m. *Step 2:* A mixture of **III** (137 mg, 0.5 mmol) and Co<sub>2</sub>(CO)<sub>8</sub> (200 mg, 0.6 mmol) was dissolved in tetrahydrofuran (3 mL). The solution was stirred at room temperature for 3 h. The desired product (**IV**) was purified by subsequent chromatography of the concentrated filtrate on silica gel with CH<sub>2</sub>Cl<sub>2</sub> as eluent. The red crystals of **IV** were recrystallized overnight from a 1:1 mixture of diethyl ether: pentane at -20°C. Yield: 60 mg (21%). <sup>1</sup>H NMR (δ in ppm, CH<sub>2</sub>Cl<sub>2</sub>): 7.30 (multiplet), -H aromatic; 6.65 (singlet), -NH; 4.35 (doublet, <sup>3</sup>J = 9.3 Hz), -CH<sub>2</sub>. IR [ $\bar{\nu}$ (CO) in cm<sup>-1</sup>, KBr disk]: 2091 s, 2055 s, 2034 s, 2017 s, 1998 s. MS (Nermag, DCI/NH<sub>3</sub>; major peaks): *m/e* 560 (M<sup>+</sup>), 548, 277.

**FT-IR Analyses.** Twenty microliters of a 10<sup>-6</sup>-10<sup>-4</sup> M (0.6-60 μg/mL) solution of **IV** in absolute ethanol were syringed onto 8 mg of dry KBr powder in a 0.5-mL Eppendorf tube. The ethanol was then stripped off by centrifugation under vacuum by using a Speed Vac concentrator (Savant, 2000 rpm) to yield a truly homogeneous mixture of the complex and KBr at the bottom of the tube. This mixture was then made into a 3-mm microdisk in the usual manner. The IR spectrum of the KBr disk was recorded in the  $\nu$ (CO) region on a Bomem Michelson 100 FT-IR spectrometer equipped with a liquid-nitrogen-cooled, indium-antimonide (In/Sb) detector. This detector is at least 10 times more sensitive in the CO stretching region than is the more commonly available mercury-cadmium-telluride (MCT) detector. The position of the KBr disk in the IR beam was adjusted by means of a 4 × beam condenser (Spectra-Bench, Spectra-Tech) in order to maximize the signal-to-noise ratios.

## RESULTS

By using the simple technique of centrifugation under vacuum to produce homogeneous solid mixtures suitable for KBr disk preparation, we could detect picomole quantities of the organocobalt complex **IV** in a reproducible manner. A representative IR spectrum of complex **IV** in the  $\nu$ (CO) region is shown in Fig. 1. Beer's law was obeyed throughout the concentration range investigated (Fig. 2). The limit of detection is approximately 10 picomoles, i.e., in the range associated with many immunological assays, especially for drugs including carbamazepine (**I**).<sup>5</sup> Our KBr-disk procedure is quite general and should prove readily applicable to many other situations where quantitative IR data on solid materials are required.

† Note: m = medium, s = strong.

## ACKNOWLEDGMENTS

This work was performed principally under the auspices of a France-Québec (Biotechnology) Exchange Grant. Operating grants in partial

support of the research) from NSERC (Canada), FCAR (Quebec), and CNRS (Région Bourgogne, France) are also gratefully acknowledged. Professor A. A. Ismail (McGill University) and Bomem are thanked for allowing us access to the Michelson 100 FT-IR spectrometer.

1. I. S. Butler, A. Vessières, and G. Jaouen, *Comments Inorg. Chem.* **6**, 269 (1989).
2. A. Vessières, S. Top, A. A. Ismail, I. S. Butler, M. Louer, and G. Jaouen, *Biochemistry* **27**, 6659 (1988).
3. A. A. Ismail, G. Jaouen, P. Cheret, and P. Brossier, *Clin. Biochem.*, in press (1989).
4. A. S. Troupin, in *Carbamazepin in Epilepsy*, H. F. Klawans, Ed. (Raven Press, New York, 1978), pp. 15-40.
5. "Hisep HPLC Direct Injection Column Provides Fast, Efficient Carbamazepine Resolution," in *Biotext* (Supelco Inc., Supelco Park, Bellefonte, Pennsylvania, 1989), Vol. 2, No. 1, 6-7.

## Quantitative, FFT-Based, Kramers-Krönig Analysis for Reflectance Data

M. L. BORTZ\* and  
R. H. FRENCH†

*E. I. DuPont de Nemours and Co., Inc., Central Research and Development Department, Experimental Station, Wilmington, Delaware 19880*

Index Headings: Computer applications; Reflectance spectroscopy; Spectroscopic techniques; UV-visible spectroscopy.

## INTRODUCTION

Kramers-Krönig analysis (KK) has been used for many years by spectroscopists to relate dissipative and dispersive processes. Traditionally, the equations have been numerically integrated according to Simpson's or MacLaurin's method, with suitable series approximations for integrating around the poles and extrapolations added to the experimentally limited data set. This implementation is usually performed on a mini or mainframe computer due to the length of the calculation, which scales as the square of the number of data points. However, the advent of 25-MHz 80386 microprocessors and Fast Fourier Transform (FFT) algorithms implemented in powerful array processing languages now allow the KK analysis to be easily performed on personal computers. The application of FFTs to KK analysis is vastly superior in computational efficiency to numerical integration, but quantitative KK analysis incorporates several subtleties, and its implementation is not straightforward. This paper discusses our implementation of quantitatively accurate FFT-based KK analysis on a 80386 processor with a 1-min run time and its performance when applied to a test function consisting of a set of Lorentz oscillators.

Received 10 May 1989.

\* Present address: Dept. of Applied Physics, Stanford University, Stanford, CA 94305.

† Author to whom correspondence should be sent.

## DISCUSSION

The familiar Kramers-Krönig dispersion relation is given by<sup>1</sup>

$$\theta(E) = \frac{-2E}{\pi} P \int_0^\infty \frac{\ln \rho(E')}{(E')^2 - E^2} dE' \quad (1)$$

in which  $\rho(E)$  is the reflected amplitude,  $\theta(E)$  is the reflected phase,  $R(E) = \rho(E)e^{i\theta(E)}$  is the complex reflectance, and  $\rho(E)^2$  is the measured reflectance; we measure a reflectance amplitude, and use the KK analysis to obtain the phase. From this we can obtain the complex dielectric constant or complex refractive index of the material through simple calculation. While the KK relation can be numerically integrated, Peterson and Knight<sup>2</sup> have shown—invoking only causality arguments—how a Fourier transform approach can be used to extract the phase from the measured reflectance. Briefly, in this approach the experimental reflectance with suitable extrapolations is transformed into Fourier space, inverted for times  $t < 0$ , and transformed back into real space. The imaginary component is then the calculated phase. The obvious advantage of this technique is it takes advantage of the computational efficiency of the FFT algorithm, which for large data sets ( $>2^{12}$ ) reduces the number of complex multiplications by two or more orders of magnitude over those required by integration techniques. With the increasing popularity of dispersive spectroscopy and the associated large data sets, this efficiency becomes increasingly important to the spectroscopist who needs PC-based analysis techniques. We have successfully modified a commercially available *qualitative* FFT-based Kramers-Krönig routine<sup>3</sup> into a *quantitatively* accurate one. There are two primary differences between our version and the commercially available one. Our version treats the extrapolations differently and also performs the analysis on data that is interpreted as even by the FFT command. This results in a quantitatively accurate KK routine.

The effect of adding extrapolations to reflectance data on the accuracy of the KK analysis is discussed extensively in the literature.<sup>4,5</sup> For all frequencies that are isolated from resonances, the reflectance is defined as

$$R = \rho^2 = \left( \frac{n-1}{n+1} \right)^2 \quad (2)$$

where  $n$  is the real part of the index of refraction. For IR data, the low-energy extrapolation is to a reflectance defined by the square root of the dc dielectric constant, and the high-energy extrapolation is to the reflectance in the visible. The values and derivatives should be continuous at the data limits. The commercially available routine mimics these extrapolations by extending the data out from their limits as two zero-slope lines of equal length, but this does not allow for continuity at the data limits, the effect of true material properties in the asymptotic limits, or the relative contributions of the unmeasured low- and high-energy regions to the phase. For visible and UV data, the extrapolations have different functional forms. The low-energy extrapolation is to the reflectance in the visible, while the high-energy extrapolation is given by  $R \propto E^{-s}$ . At photon energies above the plasma energy ( $W_p \sim 25$  eV),  $s = 4$  in the free electron

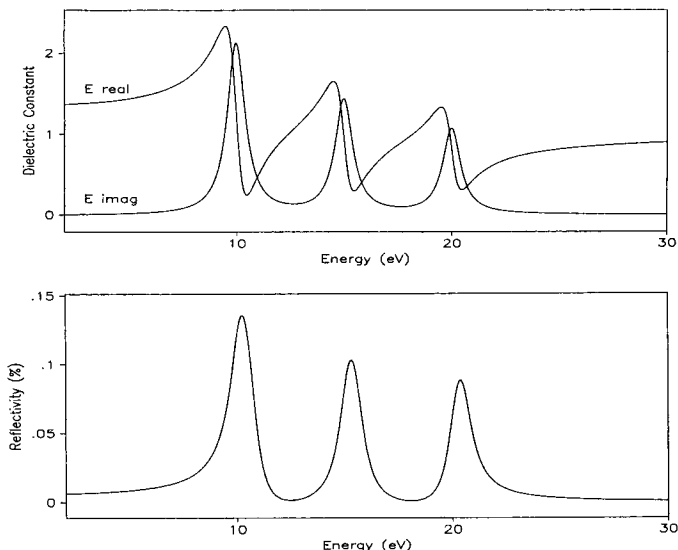


FIG. 1. Real and imaginary components of the dielectric constant and the reflectivity for a set of three Lorentz oscillators at 10, 15, and 20 eV, with equal widths and oscillator strengths.

limit. However, between the high-energy limit of visible and UV data and the plasma energy in the VUV, interband transitions continue to dominate the reflectivity, and  $E^{-s}$  extrapolation in this region is a major source of error in KK analysis of visible and UV reflectance data. Our technique adds the functionally correct extrapolations to the data.

Once the functionally correct extrapolations have been added, we invert our data through the maximum energy value, thereby doubling the size of the data set and making the data an even periodic function with respect to the Fast Fourier Transform algorithm.<sup>6</sup> This eliminates the problem of leakage, which occurs when the data to be transformed are aperiodic within the data interval, and also eliminates the imaginary component in Fourier space, since the Fourier transform of an even function is even.<sup>7</sup> We then apply the method outlined by Peterson and Knight.<sup>2</sup>

We have applied our technique to a test function consisting of three Lorentz oscillators positioned at 10, 15, and 20 eV, each with equal widths of 1 eV and equal oscillator strengths. Using an expression for the complex dielectric constant of the form

$$\epsilon_1 + i\epsilon_2 = 1 + \frac{4\pi e^2}{m} \sum_{j=1}^3 \frac{N_j}{(\omega_j^2 - \omega^2) - i\Gamma_j\omega} \quad (3)$$

we construct ideal real ( $\epsilon_1$ ) and imaginary ( $\epsilon_2$ ) components of the dielectric constant of our test function with the data extending from 2 eV to 30 eV, representing the reflectivity data range from the visible to the VUV that we obtain experimentally. From the expressions

$$n = \{ \frac{1}{2} [\sqrt{\epsilon_1^2 + \epsilon_2^2} + \epsilon_1] \}^{1/2} \quad (4)$$

$$k = \{ \frac{1}{2} [\sqrt{\epsilon_1^2 + \epsilon_2^2} - \epsilon_2] \}^{1/2} \quad (5)$$

$$R = \rho^2 = \frac{(n-1)^2 + k^2}{(n+1)^2 + k^2} \quad (6)$$

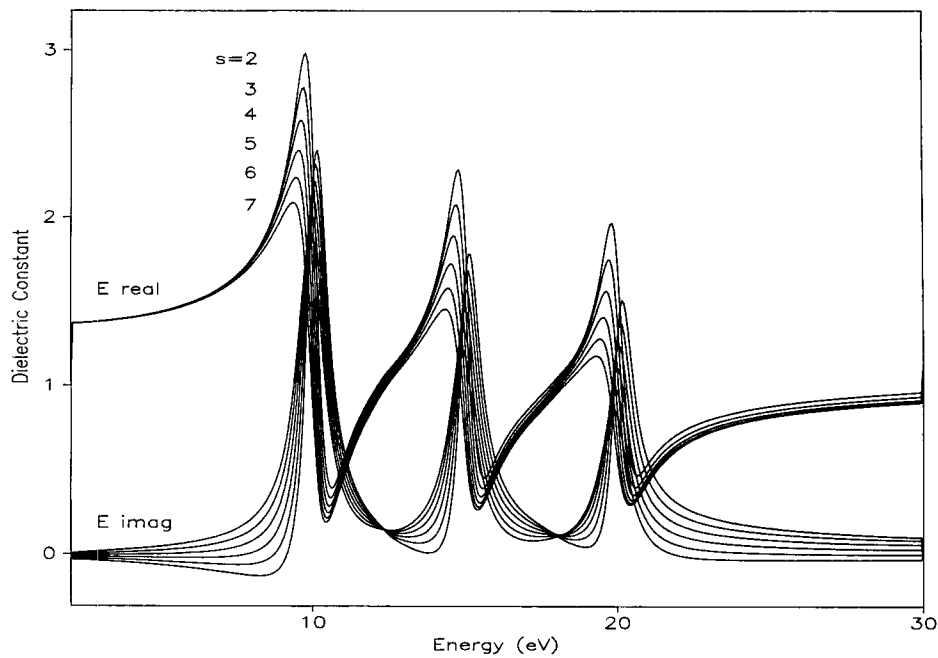


FIG. 2. Calculated real and imaginary components of the dielectric constant for different high-energy extrapolations, from  $E^{-2}$  to  $E^{-7}$ .

we obtain the ideal reflectivity from our test oscillators. Our KK analysis is performed on this reflectivity with the extrapolations added, and the calculated  $\epsilon_1$  and  $\epsilon_2$  are compared with the ideal values.

Shown in Fig. 1 are  $\epsilon_1$ ,  $\epsilon_2$ , and the reflectivity for our test oscillators. We have tested the accuracy of our technique for the functional dependence of the extrapolations, the extent of the extrapolations, and the point density of the data set. Figure 2 demonstrates the effect of changing the functional dependence of the high-energy wing while keeping its extent constant. In this case the extent of the wing was fixed at 230 eV and the func-

tional dependence swept from  $E^{-2}$  to  $E^{-7}$ . It is clear that the calculated values are swept through the correct ones as the exponent is increased from 2 to 7. Shown in Fig. 3 is the percentage error associated with the real component of the dielectric constant for high-energy extrapolation exponents between 5.6 and 6.1. In this region the calculated curves converge on the correct ones very nicely, and the error approaches 0.1% at  $s = 5.75$ . Errors of similar magnitude were observed for the imaginary component. The effect of changing the functional form of the low-energy extrapolation was investigated, and it was found that there was very little effect. A functionally

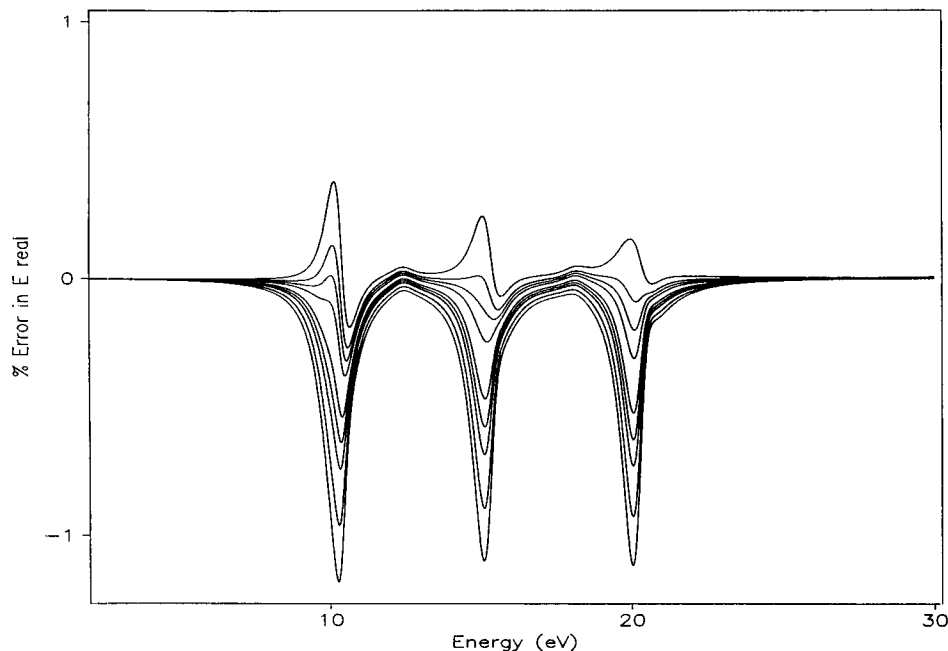


FIG. 3. Percentage error associated with the calculation of the real component of the dielectric constant for different high-energy extrapolations; errors associated with the calculation of the imaginary component are similar in magnitude.

correct extrapolation meeting the conditions of continuity was only marginally better than a straight-line extrapolation to zero energy.

We also investigated the effect of increasing the extent of the high-energy wing, while keeping its functional dependence constant. In this case the ideal  $E^{-4}$  dependence was used, and the extent swept from 100 eV to 1600 eV. While a small extrapolation of 100 eV requires a functional form of  $E^{-9}$  for reasonable accuracy, extrapolations to about 1000 eV allow the use of the physically correct  $E^{-4}$  dependence. This demonstrates the need for extrapolations of different extents, and also calls attention to the loss of point density with expanded energy ranges.

Point density obviously affects the accuracy of the FFT-based KK analysis. We examined this effect over the range of 0.006 eV/pt to 0.256 eV/pt, and found that, while the greatest point densities result in the most accurate calculations, a point density of 0.016 eV/pt was sufficiently accurate. With  $2^{14}$  data points, this implies an allowable energy range of about 260 eV. At this range, the physically correct  $E^{-4}$  dependence for the high-energy extrapolation will not provide an accurate calculation, since the energy range is too small. Thus the high-energy extrapolation is regarded as a parameter in this approach, to be iterated until the calculation becomes more accurate. In the context of performing KK analysis on real materials, known information such as the low-frequency dielectric constant, the index of refraction, or

the absorption coefficient can be used to assess the accuracy of the calculation. Because our routine is so fast, we can perform our KK analysis interactively, until we obtain consistency between all available data.

We have successfully modified a commercially available qualitative Kramers-Krönig routine into a quantitative one, and have demonstrated its accuracy with respect to a test function consisting of a set of Lorentz oscillators. The technique becomes very accurate in the limits of proper high-energy extrapolations. The accuracy of the method demonstrates a weak dependence on point density, allowing the transformations of very large data sets of over 16,000 points in about 1 min.

#### ACKNOWLEDGMENTS

The authors would like to acknowledge helpful discussions with F. A. Modine (Oak Ridge National Laboratories) and D. Kuehle (Galactic Industries).

1. See, for example, F. Wooten, *Optical Properties of Solids* (Academic Press, New York, 1972).
2. C. W. Peterson and B. W. Knight, *J. Opt. Soc. Am.* **63**, 1238 (1973).
3. *SpectraCalc*, Galactic Industries, Salem, New Hampshire.
4. F. Stern, *Solid State Physics* (Academic Press, London, 1963), Vol. 15, pp. 337-340.
5. P. O. Nilsson and L. Munkby, *Phys. Kondens. Materie.* **10**, 290 (1969).
6. K. Ohta and H. Ishida, *Appl. Spectrosc.* **42**, 952 (1988).
7. E. Brigham, *The Fast Fourier Transform* (Prentice Hall, Englewood Cliffs, New Jersey, 1974).